# The oxidation of 6-hydroxydopamine in aqueous solution. Part 2.[19] Speciation and product distribution with iron(III) as oxidant †

**Guy N. L. Jameson * ‡ and Wolfgang Linert**

*Institute of Inorganic Chemistry, Technical University of Vienna, Getreidemarkt 9/153 A-1060, Vienna, Austria. E-mail: gjameson@physics.emory.edu; wlinert@mail.zserv.tuwien.ac.at*

***Received (in Cambridge, UK) 5th September 2000, Accepted 15th February 2001***
***First published as an Advance Article on the web 20th March 2001***

6-Hydroxydopamine [5-(2-aminoethyl)benzene-1,2,4-triol, protonated form $H_3LH^+$] reacts anaerobically with aqueous iron(III) to produce four types of quinone, namely the *p*- (*p*Q), *o*- (*o*Q), triketo- (tQ) and the deprotonated quinone ($Q^-$). The relative concentrations depend strongly on the pH. At low pH *p*Q, *o*Q and tQ predominate and are in meta-stable equilibrium. However, the pH dependency of the concentrations of *p*Q and tQ at low pH suggests an equilibrium between their respective semiquinones. Above a pH of about 2, tQ disappears and above about 2.5 *p*Q and *o*Q equilibrate *via* $Q^-$, which, above a pH of about 6, is the only species present. The equilibrium constants and molar absorbances have been measured for all these species and are discussed. The speciation over the pH range 0.5–5 has been determined as a necessary prelude to a full kinetic study of the system.

## Introduction

6-Hydroxydopamine [5-(2-aminoethyl)benzene-1,2,4-triol, protonated form $H_3LH^+$§] is a catecholamine often used as a neurotoxin in animal studies to simulate Parkinson's disease,[1] a neurological disorder that affects about 1% of the population over 50 years of age. During progression of the disease, certain neurons are selectively destroyed with a concomitant increase in free iron suggesting that oxidative stress may be an important factor.[2] Furthermore, it has been shown that 6-hydroxydopamine can be formed from dopamine *via* a Fenton reaction[3] and that it can free iron from the iron storage protein ferritin.[4] It has therefore been suggested that 6-hydroxydopamine may be directly involved in the progression of the disease.[5]

Until now there have been no mechanistic studies of the oxidation of 6-hydroxydopamine by iron(III). Noradrenaline[6] [4-(2-amino-1-hydroxyethyl)benzene-1,2-diol] has been found to react *via* two parallel pathways to form the *o*-quinone, the major one *via* complex formation and the other *via* an outer-sphere mechanism. It was therefore expected that 6-hydroxydopamine would provide some interesting chemistry and indeed it has been established that it reacts with iron(III) almost exclusively *via* the outer-sphere mechanism.[5] It was also believed that a complete kinetic study of its oxidation by ferric iron might give insights into its interaction with ferritin.

The overall reaction scheme can be summarised as shown in eqn. (1).

$$\text{Catecholamine}_{(aq)} + 2\text{Fe(III)}_{(aq)} \longrightarrow \text{Quinone(s)}_{(aq)} + 2\text{Fe(II)}_{(aq)} \quad (1)$$

It has been established by NMR (see Part 1[19]) that at low pH three quinones are formed during the oxidation of 6-hydroxydopamine, an *o*-quinone (*o*Q), a *p*-quinone (*p*Q), and a triketo-quinone (tQ). All species, including the deprotonated quinone ($Q^-$), absorb in the UV or visible part of the spectrum allowing standard spectrophotometric techniques to be used to study the reaction.

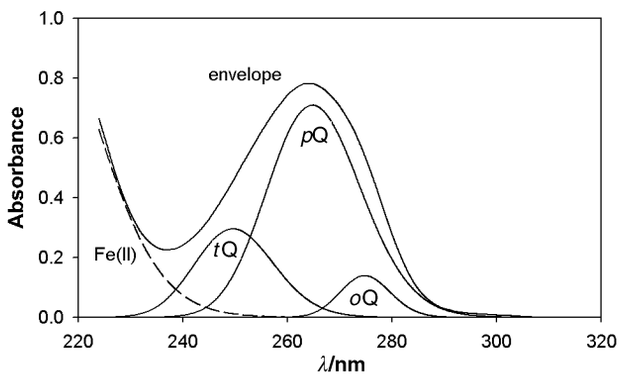


**Fig. 1** Deconvolution of the UV–Vis absorption spectrum of the products of the oxidation of 6-hydroxydopamine into Gaussian components representing the *o*-, *p*-, and triketo-quinones. (pH = 1.00, [6-hydroxydopamine] = 0.050 mM, [iron(III)] = 0.100 mM.)

It is known that both *p*- and *o*-quinones absorb in similar regions of the electronic spectrum,[7] namely a $\pi \rightarrow \pi^*$ transition at 240–300 nm, a second $\pi \rightarrow \pi^*$ transition at 285–470 nm and a weak band in the visible region. The intensity of the absorptions, however, varies enormously. *p*-Quinones absorb more strongly in the 240–300 nm region while *o*-quinones tend to absorb more strongly in the 350–400 nm region. Therefore *o*Q has a characteristic band at 390 nm while a strong absorption at 265 nm is caused by both *p*Q and tQ with a small contribution from *o*Q. A Gaussian fit (see Fig. 1) shows that indeed three species absorb in this region with maxima at 265 (*p*Q), 250 (tQ) and 275 nm (*o*Q). The molecules under study, the wavelength at which kinetic measurements were made, and their abbreviations are given in Fig. 2.

Before a plausible reaction scheme could be postulated it was necessary to establish the concentrations of the different products formed over the range of pH values studied. Furthermore, it was found that the formation of *p*Q does not follow a first-order rate law over the whole time-scale (see Part 3[20]) and only first-order reactions are concentration independent. The

† Rate constants and absorbance data are available as supplementary data. For direct electronic access see http://www.rsc.org/suppdata/p2/b0/b007162p/

‡ *Present address*: Department of Physics, Rollins Research Center, Emory University, Atlanta, GA 30322, USA.

§ For convenience, –OH protons are written to the left, and the $-NH_3^+$ proton to the right of L.

DOI: 10.1039/b007162p

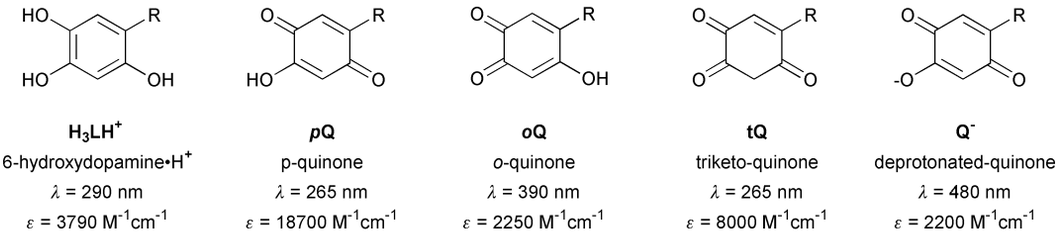


**Fig. 2** The structures and optical properties of the species investigated. (Note that the maxima quoted for *p*Q and tQ refer to the maximum of the absorption envelope and not those of the individual quinones, see text.)

molar absorbances of 6-hydroxydopamine and its quinones were therefore required.

It was also necessary to obtain the protonation constants¶ of 6-hydroxydopamine since reactions often proceed *via* a species present in minute concentrations *e.g.* a deprotonated form of the reactant. The purpose of this paper is to report the speciation and the extremely complicated product distribution of this reaction over as large a pH range as possible.

## Experimental

### (i) Chemicals

The 6-hydroxydopamine used came from two sources, Sigma-Aldrich and Fluka. 5-Hydroxydopamine [5-(2-aminoethyl)-benzene-1,2,3-triol] and dopamine [4-(2-aminoethyl)benzene-1,2-diol] were supplied by Sigma-Aldrich. Solutions of 0.1 M KOH and 0.1 M $HNO_3$ ("Tritisol" from Merck) were made up in de-ionised water, and then stored while protected by "Carbasorb" (soda lime with in-built indicator, from Merck) to stop re-absorption of $CO_2$. Solutions of $KNO_3$ (0.1 M) (Merck *pro analysi*) were made up in the same way. Iron(III) was in the form of $Fe(NO_3)_3 \cdot 9H_2O$ as supplied by Fluka (*pro analysi*).

### (ii) Potentiometric titrations

A Metler Toledo DL50 automatic titrator was used connected to an HP deskjet 500 printer. The pH electrode was initially calibrated with three buffer solutions from Riedel-de Haën or Merck (standard pHs of 4.00, 7.00 and 10.00 were employed). Samples of 6-hydroxydopamine, 5-hydroxydopamine, and dopamine, were weighed (2–4 mM) directly into 40 ml of 0.1 M $KNO_3$, previously purged with argon. These solutions were immediately titrated. All solutions were purged with argon before and during each experiment. Titrations were repeated a minimum of three times.

The results were typed into Excel for further analysis. After initial values were estimated, fitting of the data was completed with the non-linear fitting program Scientist by Micromath.

### (iii) Stopped-flow

A stopped-flow system from Applied Photo-Physics was used (SX-18MV) with PEEK valves, this flow system being designed to minimise the absorption of oxygen. The system was further prepared at the beginning of each day by purging for one hour with a 0.25 M sodium dithionite solution.

Data collection and initial manipulation were carried out on an Acorn 5000 computer using Applied Photo-Physics' own software. Further analysis of the data was completed using Excel on a PC.

6-Hydroxydopamine was always in at least a five-fold excess over iron(III) in order to achieve pseudo-(first)-order kinetics. The range of concentrations used was: for 6-hydroxydopamine 0.30–4.00 mM; and for iron(III) 0.02–0.80 mM. The ionic strength was maintained at 0.1 M with $KNO_3$.

All solutions were purged with argon and then transferred directly to the stopped-flow apparatus in gas-tight Hamilton syringes in order to prevent oxygen entering.

### (iv) pH Meter

A pH meter from Radiometer (pHM84) was used with pH electrodes from Cole-Palmer, Radiometer, and Hamilton. Initial calibration was carried out using two buffers (pH 2.00 and 7.00) obtained from either Riedel-de Haën or Merck. Further calibration of the results was achieved by using the formula established by Gorton.[8] The formula, $pH_{corr} = pH - \{0.131/(0.984pH)\}$, was verified using various concentrations of nitric acid in 0.1 M solutions of $KNO_3$.

## Results and discussion

### The protonation constants of 6-hydroxydopamine

The ease of oxidation of 6-hydroxydopamine, and indeed any trihydroxybenzene, means that accurate values for the protonation constants of 6-hydroxydopamine are extremely difficult to obtain. However to aid explanation of the kinetic data, a log $K_4$ value accurate to within ±0.05 of a log unit was all that was necessary and this was certainly achieved.

Because the protonation constants for dopamine are known accurately,[9] it was decided to include this compound to test the accuracy of our experimental set-up. The protonation constants of 5-hydroxydopamine were also measured in order that the effects of the addition of an extra –OH group to dopamine could be better understood.

By the end of each titration the solutions were usually strongly coloured (green/brown) and, in the case of 6-hydroxydopamine, accompanied by some precipitation of melanin (an organic polymer which is an end product of catecholamine oxidation). This reaction occurred despite persistent attempts to remove oxygen by purging all mixtures with argon. This partly explains the much lower precision attained for the second protonation constant. Serious discolouration is only observable above a pH of about 10 at which point oxidation can be expected to be very fast and almost certainly involves a free-radical chain reaction. Because of the danger of photolysis, light was excluded during the titration but even this precaution did not completely obviate the problem of reproducibility at high pH.

The values of log $K$ are given in Table 1. The ionisation constant of water, $pK_w$, in 0.1 M $KNO_3$ is known[10] to be 13.778 ± 0.002. The values obtained for dopamine are similar to those obtained by Kiss and Gergely[9] (13.10, 10.41, and 8.89 in 0.2 M KCl at 25 °C).

Although the protonation constants obtained are not micro-constants, those corresponding to the last three protonations of dopamine, 5-hydroxydopamine, and 6-hydroxydopamine are separated by approximately two log units and can therefore be safely assigned to –OH, $–NH_3^+$, and –OH groups respectively.

¶ Protonation constants are used throughout this work in line with compilations of data, and to be consistent with metal complex formation constants.

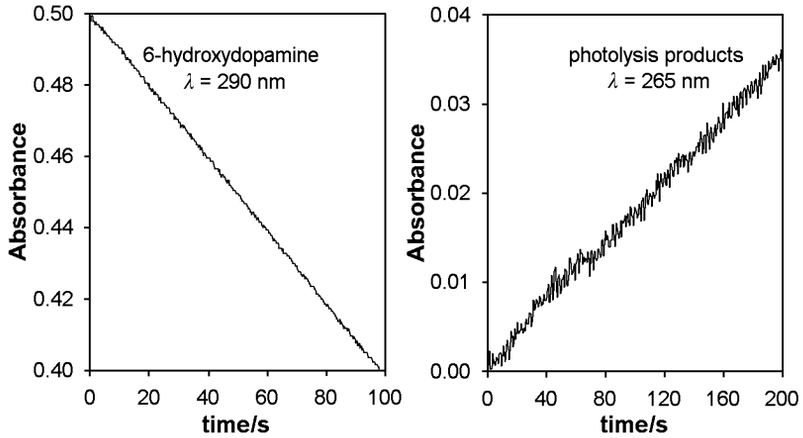


**Fig. 3** Typical photolysis absorbance–time curves.

**Table 1** Protonation constants determined for dopamine, 5-hydroxydopamine, and 6-hydroxydopamine, compared with those for phenol and catechol (0.1 M $KNO_3$, 25 °C)

| Molecule | log $K_1$ | log $K_2$ | log $K_3$ | log $K_4$ |
|---|---|---|---|---|
| Phenol[a] | 9.62 | | | |
| Catechol[a] | ~13 | 9.44 | | |
| Dopamine | 12.7 ± 0.1 | 10.44 ± 0.02 | 8.86 ± 0.03 | |
| 5-Hydroxydopamine | ∞ | 13.0 ± 0.2 | 10.78 ± 0.03 | 8.80 ± 0.02 |
| 6-Hydroxydopamine | ∞ | 12.6 ± 0.1 | 10.42 ± 0.03 | 8.88 ± 0.02 |

[a] See ref. 21.

It can be seen that the addition of a third hydroxy group changes the lowest log $K$ by very little (compare 8.86, 8.80, and 8.88). However, 5-hydroxydopamine does have a slightly lower value of this constant than either 6-hydroxydopamine or dopamine. This can be rationalised by noting that any one of the three hydroxy groups in 5-hydroxydopamine can be deprotonated to leave an internally hydrogen bonded system (see Scheme 1).

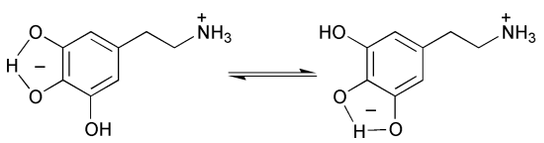

**Scheme 1** Hydrogen-bonding stabilises the loss of one proton from 5-hydroxydopamine.

The log $K_3$ values for 5-hydroxydopamine and 6-hydroxydopamine are different, the latter resembling more the log $K_2$ value of dopamine. This difference in the protonation of the $-NH_2$ group can be explained in the following way. The –OH group is inductively electron withdrawing and this effect is heightened when in the *ortho*-position. As a result, the protonation constant of the $-NH_2$ group is slightly lowered in 6-hydroxydopamine. An –OH group in the *meta*-position is electron donating leading to a higher protonation constant in 5-hydroxydopamine. This agrees with the electronic substituent constants obtained by Hammett.[11] It is interesting, however, that these effects can be seen even though the amine group is two carbon atoms away from the benzene ring. In fact, this puts into question the absolute values of micro-constants reported for dopamine and adrenaline[12] using an NMR method of assignment, relying as it does, on the remoteness of the functional groups involved.

## The photolysis of 6-hydroxydopamine

When initial attempts were made to monitor the absorption of light at 265 and 290 nm, in order to follow the formation of *p*Q and consumption of 6-hydroxydopamine respectively, it was found that the absorptions continued to change long after any chemical reaction had ceased.

Tryptophan and TOPA (2,4,5-trihydroxyphenylalanine) are light sensitive[13] below a wavelength of about 300 nm and so it was not surprising to find that 6-hydroxydopamine is also photolysed when these wavelengths are used. No attempt was made to identify the products of photolysis that also absorb below 270 nm, thus affecting the *p*Q/tQ results; nor was the mechanism investigated. Fortunately the photolysis of 6-hydroxydopamine, which is in excess, is found to be accurately zero-order (see Fig. 3) and hence a simple correction could be applied (see below).

It was decided to test whether this correction gave consistent results by measuring the molar absorbance of 6-hydroxydopamine. The absorptions of several different concentrations of 6-hydroxydopamine using two different commercially available products (Fluka and Sigma-Aldrich) were recorded over short intervals of time. These were then extrapolated to zero time. Absorptions obtained in this way were plotted, and a molar absorbance of 3790 ± 20 $M^{-1}$ $cm^{-1}$ was calculated.

## End-point analysis

As shown above, the photolysis reaction is accurately zero-order and furthermore this zero-order rate is independent of the presence of iron(III). This implied that the absorption–time curves measured at low wavelength (below 300 nm) could be corrected for photolysis by subtracting a linear absorption–time curve. Justification of the validity of this method of correction came from the treatment of the kinetic data. The reaction profile for the formation of $Q^-$ (measured at 480 nm where no photolysis is observed) reflected accurately the corrected curve for *p*Q (measured at 265 nm)—see Part 3. Fortunately the final absorptions of *o*Q and tQ could be measured at 390 and 480 nm respectively without any evidence of photolysis.

End-point absorptions could therefore be obtained over a wide range of pH values and were treated in the manner shown in eqn. (2).

$$\% \text{ species} = \frac{(\text{absorbance}/\varepsilon_{\text{species}})}{([\text{Fe}]_T/2)} \times \frac{100}{1} \qquad (2)$$

Half the total iron concentration is used because two iron atoms are needed to produce one quinone.

The data obtained in this way consisted of a series of end-point absorptions for two independently absorbing species,

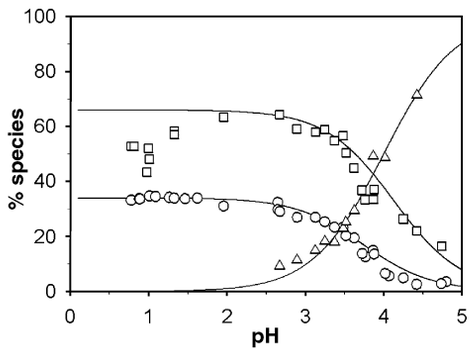


**Fig. 4** Speciation diagram (I). (○ = *o*Q; □ = *p*Q + tQ; △ = $Q^-$.)

namely *o*Q, and $Q^-$, and a combined end-point for (*p*Q + tQ). Note that all measurements of absorbance were made at 265 nm, the maximum of the observed (composite) absorption curve (see Fig. 1). The problem was converting these values to concentrations for which knowledge of the molar absorbances was required. This information is also necessary, of course, in order to analyse kinetic curves that do not exhibit first-order behaviour.

Initial values of these molar absorbances could be estimated for several of the species and compared with previously published values for analogous molecules: dopa-quinone,[14] $\lambda_{max}$ = 390 nm, $\varepsilon$ = 1650 $M^{-1}$ $cm^{-1}$; 1,4-benzoquinone,[15] $\lambda_{max}$ = 242 nm, $\varepsilon$ = 24 000 $M^{-1}$ $cm^{-1}$; $Q^-$,[16] 480 nm, $\varepsilon$ = 2700 $M^{-1}$ $cm^{-1}$.

Mure and Klinman[17] have established that the related 1,4-TOPA-quinone has a log *K* value of about 4.1. That is, the *p*-quinone is deprotonated to give a deprotonated-quinone. It is logical, therefore, to believe that the *o*Q also deprotonates to give the same species. Furthermore, this deprotonation constant would be expected to be lower because the proton cannot in this case internally hydrogen bond with an adjacent carbonyl oxygen.

NMR studies (see Part 1) have shown that at a pH of 0.7 the initial ratio of (*p*Q + tQ) to *o*Q is about 2 : 1. This, incidentally, also indicates that the ratio of the rate constants in the rate determining step, which refers to the disappearance of iron, must also be about 2 : 1 (see Part 3). Therefore at very low pH, when the quinones are in meta-stable equilibrium, the amounts of (*p*Q + tQ) and *o*Q depend upon this ratio of the rate constants. The distribution curves are thus given by eqns. (3)–(5),

$$\{oQ\} = \frac{\{oQ_{kin}\}}{(1 + 1/(K^{oQ}[H^+]))} \quad (3)$$

$$\{pQ + tQ\} = \frac{(100 - \{oQ_{kin}\})}{(1 + 1/(K^{pQ}[H^+]))} \quad (4)$$

$$\{Q^-\} = 100 - (\{oQ\} + \{pQ + tQ\}) \quad (5)$$

where {*o*Q} is the percentage of *o*Q *etc.*; $\{oQ_{kin}\}$ is the kinetically determined percentage of *o*Q when it is in meta-stable equilibrium and $K^{oQ}$ and $K^{pQ}$ are the protonation constants defined in Table 4.

Estimates of the molar absorbances were used to convert the data to percentages according to eqn. (2). The molar absorbances and the protonation constants were then varied until the points and the theoretical distribution curves agreed with each other. The inter-dependence of the various constants, and the shapes of the curves when equilibrium between the quinones *via* $Q^-$ occurs, meant that there was very little freedom as to which values were accepted. The data points and theoretical curves are given in Fig. 4. The best fit was obtained with a (*p*Q + tQ) to *o*Q ratio of 1.94 : 1 (±0.02).

**Protonation of the *p*-semiquinone**

One discrepancy, however, is evident. The data points pertaining to the sum of *p*Q and tQ decrease at low pH and yet the NMR experiments show the quinones are in meta-stable equilibrium. Any pH-dependency of the quinones must therefore arise through protonic equilibrium between their semiquinones. It has been shown in Part 1 that the product distribution is oxidant independent suggesting that the transition state is more "product-like", giving a pH dependent constant ratio of concentrations of the three semiquinones. This arises from the distribution of the unpaired electron and proton over the molecular skeleton and further implies that any equilibrium between the three semiquinones is slow enough to allow the second oxidation step to take place without further change in distribution.

This can be expressed in terms of protonation of the *p*-semiquinone (*p*sq) which is assumed to give rise to the triketo-semiquinone (tsq) alone, the other species similarly giving rise to the irreversible formation of their respective quinones, see Scheme 2.

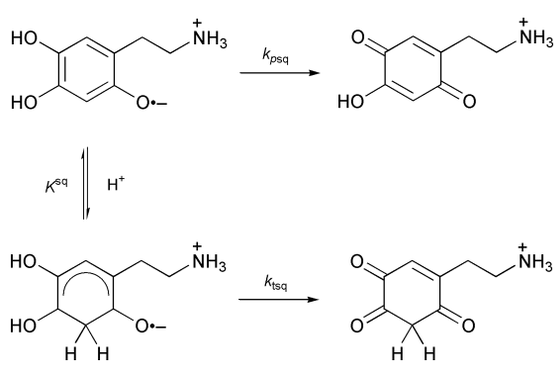


**Scheme 2** Protonation equilibria involved between the *p*- and triketo-semiquinones.

From this scheme, the rates of formation of the quinones are given by eqns. (6) and (7).

$$\frac{d[pQ]}{dt} = k_{psq}[psq] \quad (6)$$

$$\frac{d[tQ]}{dt} = k_{tsq}[tsq] = k_{tsq}K^{sq}[H^+][psq] \quad (7)$$

We can assume that the ratio of the final products equals the ratio of the rates of their formation [eqn. (8)].

$$\left\{\frac{d[tQ]}{dt} \Big/ \frac{d[pQ]}{dt}\right\} = \frac{k_{tsq}K^{sq}[H^+]}{k_{psq}} = \frac{[tQ]_{final}}{[pQ]_{final}} = K^{eff}[H^+] \quad (8)$$

This protonation constant, $K^{eff}$, would be expected to be quite small and this would explain why tQ is not observed at higher pHs. The molar absorbance so far obtained for the peak at 265 nm (18 700 $M^{-1}$ $cm^{-1}$) is therefore that for *p*Q alone and the molar absorbance for tQ was therefore required.

Analogous experiments using sodium periodate as the oxidant were examined using both NMR and UV–Vis spectroscopy. Because it can be assumed that the NMR data correctly reflect the proportions of the quinones, the percentages of the quinones present are as listed in Table 2. Knowing the molar absorbances of *o*Q and *p*Q and accepting 10.7 as the percentage of the *p*Q enables the molar absorbance of tQ to be calculated. A value of 8000 $M^{-1}$ $cm^{-1}$ was accepted and the excellent overall agreement between the NMR and UV–Vis data based on this assignment is shown in Table 2.

The data points lying below the theoretical *p*Q curve in Fig. 4

**Table 2** The speciation produced by the oxidation of 6-hydroxydopamine with sodium periodate: comparison of NMR and UV–Vis results

| Quinone | $\lambda$/nm | $\varepsilon$/M$^{-1}$ cm$^{-1}$ | % species | |
|---|---|---|---|---|
| | | | UV–Vis | NMR |
| *o*Q | 390 | 2 250 ± 10 | 30.7 | 30.9 |
| *p*Q | 265 | 18 700[a] ± 100 | 58.7 | 58.4 |
| tQ | 265 | 8 000[a] ± 100 | 10.7[b] | 10.7 |

[a] These values apply to measurements made at the envelope absorption maximum of 265 nm. [b] NMR value accepted as correct.

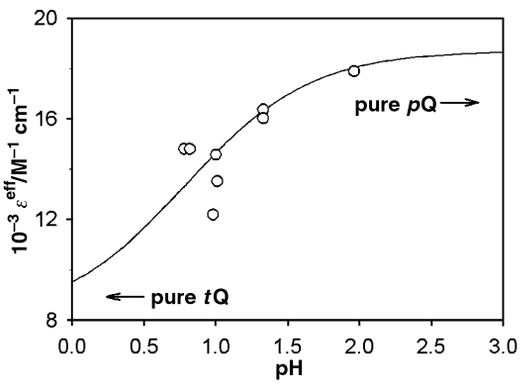


**Fig. 5** Determination of the *apparent* protonation constant for the triketo-quinone, a value of log $K^{eff} = 0.78$ was accepted.

can now be corrected assuming a contribution from tQ. This has been done by first assigning an effective molar absorbance $\varepsilon^{eff}$ [eqn. (9)] to each end-point absorbance so that the data

$$([pQ] + [tQ])\varepsilon^{eff} = [pQ]\varepsilon^{pQ} + [tQ]\varepsilon^{tQ} \quad (9)$$

points lie on the theoretical curve [eqn. (4)] that refers to the sum of the two.

These effective molar absorbances can then be fitted to a protonation curve where the limits at either end refer to the molar absorbances of the pure substances, given in Table 2 [eqn. (10)].

$$\varepsilon^{eff} = \frac{\{\varepsilon^{pQ} + K^{eff}[H^+]\varepsilon^{tQ}\}}{\{1 + K^{eff}[H^+]\}} \quad (10)$$

This is illustrated in Fig. 5; a value of log $K^{eff} = 0.78$ was accepted. Note that this constant, $K^{eff}$, is only an apparent equilibrium constant that includes the ratio of the rate constants of the two reactions. The scatter in the results at low pH is unavoidable because of (a) the difficulty in measuring accurately the pH at these low values and (b) an increase in the importance of the photolysis reaction.

Using this value for $K^{eff}$, the variation of the concentration of tQ with pH could be calculated. This enabled the low pH points obtained at 265 nm to be corrected to give the sum of the two percentages (*p*Q + tQ). Theoretical curves for tQ and *p*Q could also be drawn using the constants obtained [eqns. (11) and (12)] thus completing the speciation diagram, Fig. 6. The molar

$$\{pQ\} = \frac{(100 - \{oQ_{kin}\})}{(1 + K^{eff}[H^+])(1 + 1/K^{pQ}[H^+])} \quad (11)$$

$$\{tQ\} = \{pQ + tQ\} - \{pQ\} \quad (12)$$

absorbances established in this way are listed in Table 3, and the equilibrium constants used are given in Table 4.

**Table 3** Molar absorbances obtained

| Quinone | $\lambda$/nm | $\varepsilon$/M$^{-1}$ cm$^{-1}$ |
|---|---|---|
| *o*Q | 390 | 2 250 ± 10 |
| *p*Q | 265 | 18 700 ± 100 |
| tQ | 265 | 8 000 ± 100 |
| $Q^-$ | 480 | 2 200 ± 10 |

**Table 4** The equilibrium constants employed

| Equilibrium | Symbol | log *K* |
|---|---|---|
| $Q^- + H^+ \rightleftharpoons oQ$ | $K^{oQ}$ | 3.74 ± 0.02 |
| $Q^- + H^+ \rightleftharpoons pQ$ | $K^{pQ}$ | 4.13 ± 0.02 |

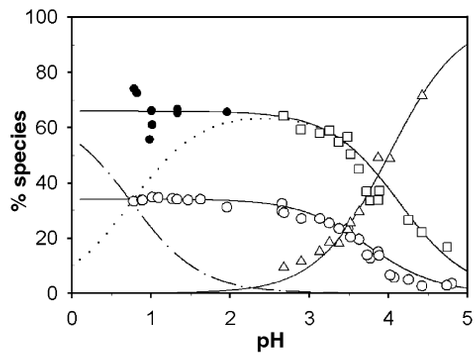


**Fig. 6** Speciation diagram (II). ○ = *o*Q; □ = *p*Q; △ = deprotonated-quinone $Q^-$; ● = sum of *p*Q and tQ; ····· = *p*Q (calculated) –·–·– = tQ (calculated).

Because 6-hydroxydopamine does not form a stable complex,[5] the irreversible precipitation of iron(III) hydroxide above a pH of about 5 makes the results unreliable and therefore these investigations could not be extended beyond this point. Note that 6-hydroxydopamine does react slowly with this insoluble form of iron as is observed when following the kinetics of its interaction with ferritin.[18]

### Interpretation of the product distribution curves

It should be noted that at low pHs (up to about 3) the system is not in equilibrium. Fig. 6 therefore illustrates the *initial* product distribution. The products are *meta-stable* and react further, by means of a ring-closure of the amine side-chain with carbonyl 6 in the case of *p*Q, before they can inter-convert (see Part 1). However, if the pH is increased to above about 3, the quinones inter-convert *via* $Q^-$ and thus reach equilibrium. The ratio of *p*Q to *o*Q *at equilibrium* therefore reaches a value of $K^{pQ}/K^{oQ} = 10^{4.13}/10^{3.74} = 2.45$. As the pH is further increased *o*Q and *p*Q eventually disappear as they convert into $Q^-$ but the ratio of *p*Q : *o*Q is pH independent up to this point.

## Conclusions

It can be seen that the product distribution of 6-hydroxydopamine oxidation by iron(III) is complicated and strongly pH-dependent. At pH < 2 the inter-conversion of the three quinones formed is extremely slow (see Part 1). At physiological pHs only the highly coloured deprotonated quinone, $Q^-$, is produced.


## Acknowledgements

The authors wish to thank the "Fonds zur Förderung der wissenschaftlichen Forschung" (FWF) (Project No. 11218-

CHE), and the Austrian Federal Ministry of Science and Transport (Project No. GZ 70.023/2-Pr/4/97). This project was also supported by the "Österreichische Nationalbank" (Project No. 5556). We would further like to thankfully acknowledge the support of this project *via* the EU COST project D8 (Chemistry of Metals in Medicine) and the TMR project (TOSS) supported by the European Community under the Contract number ERB-FMRX-CT98-0199.

## References

1 M. Gerlach and P. J. Riederer, *J. Neural Transm.*, 1996, **103**, 987.
2 G. N. L. Jameson and W. Linert, in *Free Radicals in Brain Pathophysiology*, ed. G. Poli, E. Cadenas and L. Packer, Marcel Dekker, New York, 2000, p. 247.
3 Z. Maskos, J. D. Rush and W. H. Koppenol, *Arch. Biochem. Biophys.*, 1992, **296**, 514; Z. Maskos, J. D. Rush and W. H. Koppenol, *Arch. Biochem. Biophys.*, 1992, **296**, 521.
4 H. P. Monteiro and C. C. Winterbourn, *Biochem. Pharmacol.*, 1989, **38**, 4177; K. L. Double, M. Maywald, M. Schmittel, P. Riederer and M. Gerlach, *J. Neurochemistry*, 1998, **70**, 2492.
5 W. Linert, E. Herlinger, R. F. Jameson, E. Kienzl, K. Jellinger and M. B. H. Youdim, *Biochim. Biophys. Acta*, 1996, **1316**, 160.
6 U. El-Ayaan, R. F. Jameson and W. L. Linert, *J. Chem. Soc.*, *Dalton Trans.*, 1998, 1315.
7 S. Berger and A. Rieker, in *The Chemistry of Quinonoid Compounds*, ed. S. Patai and Z. Rappoport, Wiley, New York, 1988, vol. 2, ch. 4.
8 J. E. Gorton, PhD Thesis, University of St. Andrews, Scotland, 1968.
9 T. Kiss and A. Gergely, *Inorg. Chim. Acta*, 1979, **36**, 31.
10 R. F. Jameson and M. F. Wilson, *J. Chem. Soc.*, *Dalton Trans.*, 1972, 2607.
11 L. P. Hammett, *Physical Organic Chemistry*, McGraw-Hill, New York, 1970.
12 R. F. Jameson, G. Hunter and T. Kiss, *J. Chem. Soc.*, *Perkin Trans. 2*, 1980, 1105.
13 Dr S. Senior, Applied Photophysics, personal communication.
14 W. Linert, R. F. Jameson and E. Herlinger, *Inorg. Chim. Acta*, 1991, **187**, 239.
15 D. H. Williams and I. Fleming, *Spectroscopic Methods in Organic Chemistry*, McGraw-Hill Book Company, London, 1980.
16 G. A. Swan, *J. Chem. Soc.*, *Perkin Trans. 1*, 1976, 339.
17 M. Mure and J. P. Klinman, *J. Am. Chem. Soc.*, 1993, **115**, 7117.
18 G. N. L. Jameson, R. F. Jameson and W. Linert, unpublished work.
19 Part 1. G. N. L. Jameson, A. B. Kudryavtsev and W. Linert, *J. Chem. Soc.*, *Perkin Trans. 2*, 2001 (DOI: 10.1039/b007912j).
20 Part 3. G. N. L. Jameson and W. Linert, *J. Chem. Soc.*, *Perkin Trans. 2*, 2001 (DOI: 10.1039/b007203f).
21 *Stability Constants of Metal-Ion Complexes*, ed. L. G. Sillen and A. E. Martell, The Chemical Society, London, Special publications 17 and 25, 1964.